

## Weak Pseudogap Behavior in the Underdoped Cuprate Superconductors

Jörg Schmalian,<sup>1</sup> David Pines,<sup>1,2</sup> and Branko Stojković<sup>2</sup>

<sup>1</sup>University of Illinois at Urbana-Champaign, Loomis Laboratory of Physics, 1110 W. Green, Urbana, Illinois 61801

<sup>2</sup>Center for Nonlinear Studies, Los Alamos National Laboratory, Los Alamos, New Mexico 87545

(Received 4 August 1997)

We report on a novel solution of the nearly antiferromagnetic (AF) spin fermion model in the limit  $\pi T \gg \omega_{\text{sf}}$ , which demonstrates that the broad high energy features found in angular resolved photoemission spectroscopy measurements of the spectral density of the underdoped cuprates are determined by strong (AF) correlations and precursor effects of a spin density wave state. We show that the onset temperature,  $T^{\text{cr}}$ , of weak pseudogap behavior is determined by the strength,  $\xi$ , of the (AF) correlations, and obtain the generic changes in low frequency magnetic behavior seen in NMR experiments with  $\xi(T^{\text{cr}}) \approx 2$ , confirming the Barzykin and Pines crossover criterion. [S0031-9007(98)05982-1]

PACS numbers: 74.25.Ha

Magnetically underdoped cuprates may be distinguished from their overdoped counterparts by the presence of a maximum at a temperature  $T^{\text{cr}} > T_c$  in the temperature dependent uniform susceptibility,  $\chi_o(T)$ . They are characterized by the occurrence of a quasiparticle pseudogap observed by nuclear magnetic resonance (NMR) and inelastic neutron scattering experiments, optical, transport, and specific heat measurements, and in angular resolved photoemission spectroscopy (ARPES). Barzykin and Pines [1] proposed that at  $T^{\text{cr}}$ , sizable antiferromagnetic (AF) correlations between the planar quasiparticles bring about a change in the spin dynamics, and that at  $T$  near  $T^{\text{cr}}$ , the quantity  ${}^{63}\text{T}_1 T / {}^{63}\text{T}_{2\text{G}}^2$ , where  ${}^{63}\text{T}_1$  is the  ${}^{63}\text{Cu}$  spin-lattice relaxation time and  ${}^{63}\text{T}_{2\text{G}}$  is the spin-echo decay time, changes from being nearly independent of temperature (above  $T^{\text{cr}}$ ), to a quantity which varies as  $(a + bT)^{-1}$ . This behavior has recently been confirmed in NMR measurements by Curro *et al.* [2]. Since  ${}^{63}\text{T}_1 T / {}^{63}\text{T}_{2\text{G}}^2 \propto \xi^{n-z}$ , where  $z$  is a dynamical exponent [1], the near temperature independence of  ${}^{63}\text{T}_1 T / {}^{63}\text{T}_{2\text{G}}^2$  found between  $T^{\text{cr}}$  and a lower crossover temperature,  $T_*$ , suggests that one is in a pseudoscaling regime ( $z \approx 1$ ), while the temperature independence of  ${}^{63}\text{T}_1 T / {}^{63}\text{T}_{2\text{G}}^2$  above  $T^{\text{cr}}$  suggests mean field behavior ( $z \approx 2$ ). Moreover, above  $T_*$  ARPES experiments show that the spectral density of quasiparticles located near  $(\pi, 0)$  has developed a high energy feature [3]. We refer to this behavior as *weak pseudogap behavior*, to distinguish it from the *strong pseudogap behavior* found below  $T_*$ , where experiment shows a leading edge gap develops in the quasiparticle spectrum [3]. Strong pseudogap behavior is also seen in specific heat, dc transport, and optical experiments, while  ${}^{63}\text{T}_{2\text{G}}$  measurements show that the AF spin correlations become frozen (i.e.,  $\xi \approx \text{const}$ ) and  ${}^{63}\text{T}_1 T$  displays gaplike behavior.

The nearly antiferromagnetic Fermi liquid (NAFL) model [4,5] of the cuprates offers a possible explanation for the observed weak and strong pseudogap behavior. In this model, changes in quasiparticle behavior both reflect

and bring about the measured changes in spin dynamics. The highly anisotropic effective planar quasiparticle interaction mirrors the dynamical spin susceptibility, peaked near  $\mathbf{Q} = (\pi, \pi)$ , introduced by Millis, Monien, and Pines (MMP) [6] to explain NMR experiments,

$$V_{\text{eff}}^{\text{NAFL}}(\mathbf{q}, \omega) = g^2 \chi_{\mathbf{q}}(\omega) = \frac{g^2 \chi_{\mathbf{Q}}}{1 + \xi^2 (\mathbf{q} - \mathbf{Q})^2 - i \frac{\omega}{\omega_{\text{sf}}}}, \quad (1)$$

where  $\chi_{\mathbf{Q}} = \alpha \xi^2$ , with  $\alpha$  constant, and  $g$  is the coupling constant.

Since the dynamical spin susceptibility  $\chi_{\mathbf{q}}(\omega)$  peaks at wave vectors close to  $(\pi, \pi)$ , two different kinds of quasiparticles emerge: *hot quasiparticles*, located close to those momentum points on the Fermi surface which can be connected by  $\mathbf{Q}$ , feel the full effects of the interaction of Eq. (1); *cold quasiparticles*, located not far from the diagonals,  $|k_x| = |k_y|$ , feel a “normal” interaction. Their distinct lifetimes can be inferred from transport experiments, where a detailed analysis shows that the behavior of the hot quasiparticles is highly anomalous, while cold quasiparticles may be characterized as a strongly coupled Landau Fermi liquid [7].

In the present Letter, we focus our attention on temperatures  $T \geq T_*$ . Our reason for doing so is that, for  $T > T_*$ , fits to NMR experiments show that  $\omega_{\text{sf}} < \pi T$  [ $\omega_{\text{sf}}/(\pi T) \approx 0.17$  for  $\text{YBa}_2\text{Cu}_4\text{O}_8$  and  $\omega_{\text{sf}}/(\pi T) \approx 0.14$  for  $\text{YBa}_2\text{Cu}_3\text{O}_{6.63}$  [1]]. Hence the spin system is thermally excited and behaves quasistatically; the hot quasiparticles see a spin system which acts like a static deformation potential, a behavior which is no longer found below  $T_*$  where  $\omega_{\text{sf}}$  increases rapidly [1] and the lowest scale is the temperature itself. In the limit  $\pi T \gg \omega_{\text{sf}}$  it is possible to sum the entire perturbation series (all diagrams) of the two dimensional spin fermion model with the effective interaction,  $V_{\text{eff}}^{\text{NAFL}}(\mathbf{q}, \omega)$ , of Eq. (1).

Our main results are the appearance (along with its momentum dependence) in the hot quasiparticle spectrum

of the high energy features seen in ARPES, a maximum in  $\chi_o(T)$ , and a crossover in  ${}^{63}\text{Tl}T/{}^{63}\text{Tl}T_{2G}^2$  for  $\xi > \xi_o \approx v_F/\Delta_o$  seen in NMR. These result from the emergence of a spin density wave (SDW)-like state, as proposed by Chubukov *et al.* [8]. Here,  $v_F$  is the Fermi velocity and  $\Delta_o = \frac{g}{\sqrt{3}}\sqrt{\langle \mathbf{S}^2 \rangle} \sim \frac{g}{2}$ , a characteristic energy scale of the SDW-like pseudogap. Using typical values for the hopping matrix elements (see below), and  $g \approx 0.6$  eV (determined from the analysis of transport experiments in slightly underdoped materials [7]), we find  $\xi_o \approx 2$ . For  $\xi > \xi_o$ , the hot quasiparticle spectral density reflects the emerging spin density wave state, while the MMP interaction generates naturally the distinct behavior of hot and cold quasiparticle states seen in ARPES experiments.

We summarize our calculations briefly. Using the effective interaction, Eq. (1), the direct spin-spin coupling is eliminated via a Hubbard-Stratonovich transformation, introducing a collective spin field  $\mathbf{S}_q(\tau)$ . After integrating out the fermionic degrees of freedom, the single particle Green's function can be written as

$$G_{\mathbf{k},\sigma}(\tau - \tau') = \langle \hat{G}_{\mathbf{k},\mathbf{k}\sigma\sigma}(\tau, \tau' | \mathbf{S}) \rangle_o, \quad (2)$$

where  $\hat{G}_{\mathbf{k},\mathbf{k}\sigma\sigma}(\tau, \tau' | \mathbf{S})$  is the matrix element of

$$\left[ G_{o\mathbf{k}}^{-1}(\tau - \tau')\delta_{\mathbf{k},\mathbf{k}'} - \frac{g}{\sqrt{3}} \mathbf{S}_{\mathbf{k}-\mathbf{k}'}(\tau)\delta(\tau - \tau') \cdot \vec{\sigma} \right]^{-1}, \quad (3)$$

which describes the propagation of an electron for a given configuration  $\mathbf{S}$  of the spin field.  $\vec{\sigma}$  is the Pauli matrix vector, and  $G_{o\mathbf{k}} = -(\partial_\tau + \varepsilon_{\mathbf{k}})^{-1}$  is the bare single particle Green's function with bare dispersion  $\varepsilon_{\mathbf{k}} = -2t(\cos k_x + \cos k_y) - 4t' \cos k_x \cos k_y - \mu$ . We use  $t = 0.25$  eV and  $t' = -0.25t$  for the nearest and next nearest neighbor hopping integrals, respectively, and adjust the chemical potential  $\mu$  to maintain the hole concentration at  $n_h$ . The average  $\langle \dots \rangle_o \propto \int \mathcal{D}\mathbf{S} \dots \exp\{-S_o\}$  is performed with respect to the action of the collective spin degrees of freedom,

$$S_o(\mathbf{S}) = \frac{T}{2} \sum_{\mathbf{q},n} \chi_{\mathbf{q}}^{-1}(i\omega_n) \mathbf{S}_{\mathbf{q}}(i\omega_n) \cdot \mathbf{S}_{-\mathbf{q}}(-i\omega_n), \quad (4)$$

where  $\omega_n = 2n\pi T$ . In using Eq. (2) we have assumed that (i)  $\chi_{\mathbf{q}}(\omega)$  is the fully renormalized spin susceptibility taken from the experiment and (ii) any nonlinear (higher order in  $\mathbf{S}$  than quadratic) terms of the spin field can be neglected. The model which results from assumption (ii) is usually referred to as the spin fermion model.

After inversion of Eq. (3) in spin space, the average of Eq. (2) can be evaluated diagrammatically using Wick's theorem for the spin field. In the static limit,  $\pi T \gg \omega_{\text{sf}}$ , it suffices to consider only the zeroth bosonic Matsubara frequency in  $\chi_{\mathbf{q}}(i\omega_n)$ . This follows from Eq. (1) after analytical continuation and is also reflected in the fact that the second order diagram, which is particularly important for smaller doping concentrations [9], is dominated by the lowest Matsubara frequency if  $\pi T \gg \omega_{\text{sf}}$ . The remaining momentum summations are

evaluated by expanding  $\varepsilon_{\mathbf{k}+\mathbf{q}} \approx \varepsilon_{\mathbf{k}+\mathbf{Q}} + \mathbf{v}_{\mathbf{k}+\mathbf{Q}} \cdot (\mathbf{q} - \mathbf{Q})$  for momentum transfers close to  $\mathbf{Q}$ , an approximation which, as explicit calculations show, is justified for  $\xi > 1$ . Here  $v_{\mathbf{k}+\mathbf{Q}}^\alpha = \partial \varepsilon_{\mathbf{k}+\mathbf{Q}} / \partial k_\alpha$ . In this limit *all diagrams* can be summed up by generalizing a solution for a one dimensional charge density wave system obtained by Sadovskii [10] to the case of two dimensions and, more importantly, to isotropic spin fluctuations. In detail, the solution consists of two steps: First, for  $\omega_{\text{sf}} \ll \pi T$  each crossing diagram of the spin fermion model equals, besides sign and multiplicity, a particular noncrossing diagram. Second, we determine the total,  $\xi$  independent multiplicity of each class of identical diagrams from the straightforward solution in the limit  $\xi \rightarrow \infty$ , taking care to ensure spin rotation invariance.

We find the following recursion relation for the Green's function  $G_{\mathbf{k}}(\omega) \equiv G_{\mathbf{k}}^{(l=0)}(\omega)$ , whose imaginary part determines the spectral density  $A(\mathbf{k}, \omega)$ :

$$G_{\mathbf{k}}^{(l)}(\omega)^{-1} = g_{\mathbf{k}}^{(l)}(\omega)^{-1} - \kappa_{l+1} \Delta_o^2 G_{\mathbf{k}}^{(l+1)}(\omega). \quad (5)$$

Here,  $\kappa_l = (l+2)/3$  if  $l$  is odd, while  $\kappa_l = l/3$  if  $l$  is even, and  $g_{\mathbf{k}}^{(l)}(\omega)$  is the Fourier transform of  $-i\Theta(t)e^{-i\varepsilon_{\mathbf{k}+\mathbf{Q}}t} [K_0(t|\mathbf{v}_{\mathbf{k}+\mathbf{Q}}|/\xi)/(2\pi)]^l$  with modified Bessel function  $K_0(x)$ . The recursion relation, Eq. (5), closed by  $G_{\mathbf{k}}^{(L)}(\omega) = g_{\mathbf{k}}^{(L)}(\omega)$  for some large value of  $L$ , enables us to calculate  $A(\mathbf{k}, \omega)$  to arbitrary order  $2L$  in the coupling constant  $g$  [we use  $L \sim 10^3$ ; Eq. (5) converges for  $L \sim 10^2$ ]. For simplicity, we use in the following the approximation  $K_0(x) \approx 2\pi e^{-x}$ . We have checked numerically that this approximation does not change any conclusion of this paper. In the limit  $\xi \rightarrow \infty$  the Green's function reduces to  $G_{\mathbf{k}}(\omega) = \int d\Delta p(\Delta) G_{\mathbf{k}}^{\text{SDW}}(\Delta)$ , where  $G_{\mathbf{k}}^{\text{SDW}}(\Delta)$  is the single particle Green's function of the mean field SDW state and  $p(\Delta) \sim \Delta^2 \exp(-\frac{3}{2}\Delta^2/\Delta_o^2)$  is the distribution function of a fluctuating SDW gap, centered around  $\sqrt{\frac{2}{3}}\Delta_o$ ; i.e., the amplitude fluctuations

of the spins  $\mathbf{S}$  are confined to a region around  $\sqrt{\frac{2}{3}}\langle \mathbf{S}^2 \rangle$ , although in our calculations directional fluctuations are fully isotropic and spin rotation invariance is maintained. Below we show that the SDW-like solution is obtained even at finite values of  $\xi$ .

The quantities we calculate are the single particle spectral density,  $A(\mathbf{k}, \omega)$ , and the low frequency behavior of the irreducible spin susceptibility  $\tilde{\chi}_{\mathbf{q}}(\omega, T)$ . In Fig. 1(a), we show our results for the product of  $A_{\mathbf{k}}(\omega)$  and the Fermi function,  $f(\omega)$ , which demonstrate the qualitatively different behavior of hot quasiparticles close to  $(\pi, 0)$  and cold quasiparticles close to the diagonals  $|k_x| = |k_y|$ . We see that in contrast to the conventional behavior of the cold quasiparticles, whose spectral function is peaked at the Fermi energy, the hot quasiparticle density of states develops a pronounced high energy feature (peak) as observed in experiments [3,11]. Although the hot quasiparticles do not possess a distinct peak at the Fermi

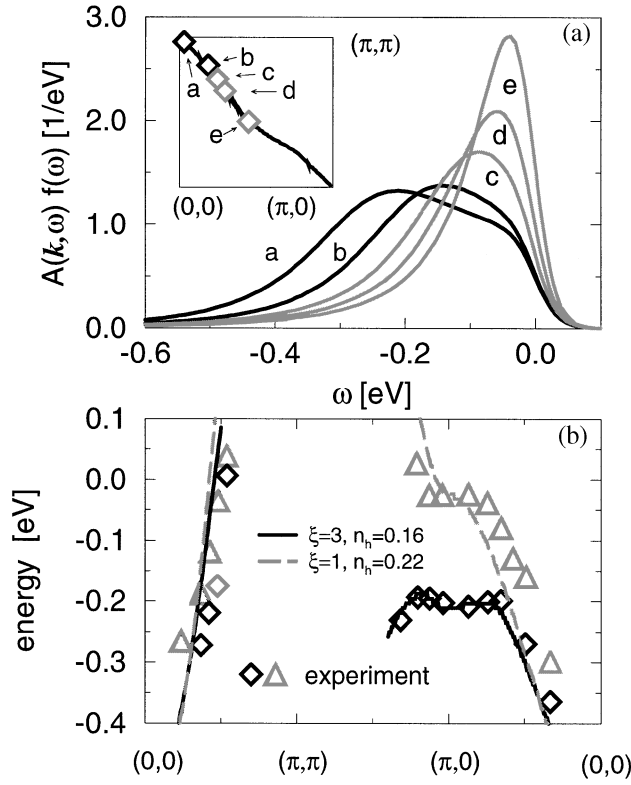


FIG. 1. (a) Spectral density multiplied with Fermi function on the Fermi surface for  $\xi = 3$ . The distinct behavior of hot and cold quasiparticles is visible. The inset shows the corresponding Fermi surface. (b) Momentum dependence of local maxima of the spectral density as a function of  $\xi$  and hole doping concentration  $n_h$  is compared with experiments of Ref. [11] for  $\text{Bi}_2\text{Sr}_2\text{Ca}_{1-x}\text{Dy}_x\text{Cu}_2\text{O}_{8+\delta}$  with  $x = 0.01$  (triangles) and  $x = 0.175$  (diamonds). Only maxima with relative spectral weight  $>10\%$  are shown.

level, due to their strong scattering rates, this does not mean that the system has lost pieces of the Fermi surface; rather we find that the Fermi surface, defined by  $\varepsilon_{\mathbf{k}} + \text{Re} \Sigma_{\mathbf{k}}(\omega = 0) = 0$ , remains large but the coherent peak at the Fermi energy falls below the visibility threshold of present ARPES experiments. Even though these coherent quasiparticles are invisible in the present temperature range, they are, we believe, responsible for the sharp peak for  $\mathbf{k} \sim (\pi, 0)$ , observed in ARPES below the superconducting transition temperature [3] where the low frequency scattering rate is strongly suppressed. It is only for  $\xi > 30$ , which is not appropriate for the underdoped cuprates studied here, that the solution of Eq. (5) yields hole pockets, closed around  $(\pi/2, \pi/2)$ , accompanied by a large piece of a Fermi surface (FS) closed around  $(0,0)$  [9]. If one determines the  $\mathbf{k}$  states for which the occupation number  $n_{\mathbf{k}} = \frac{1}{2}$ , the resulting line in momentum space can hardly be distinguished from the uncorrelated FS; i.e., the total occupied spectral weight of a given momentum state is quite robust with respect to the drastic changes of the line shape of the spectral function. There-

fore, high energy features are always more pronounced for the occupied part of the density of states than for its unoccupied part, since states close to  $(\pi, 0)$  remain mostly occupied.

In Fig. 1(b) we compare our results for the momentum dependence of the high energy features with the experimental results of Marshall *et al.* [11] for two different doping concentrations. The best agreement between theory and experiment was obtained for a next nearest neighbor hopping element  $t' = -0.25t$ . It can be seen that within our approach one can understand the qualitatively different behavior experimentally seen for underdoped and overdoped systems, as well as the detailed momentum dependence of the high energy features in the underdoped case. While for overdoped cuprates the FS crossing close to  $(\pi, 0)$  is clearly visible, no such crossing has been observed in the underdoped systems. In contrast, along the diagonal of the Brillouin zone, there is little difference in the behavior of underdoped and overdoped systems. This detailed agreement between theory and experiment is a strong indication that the high energy features of cuprate superconductors seen in ARPES experiments are indeed due to precursors of a SDW-like state.

We sum *all diagrams* of the perturbation series for the electron-spin fluctuation vertex function  $\Gamma \equiv \Gamma^{(0)}$  in similar fashion as the Green's function  $G_{\mathbf{k}}(\omega)$  in Eq. (5) and find

$$\begin{aligned} \Gamma_{\mathbf{k}, \mathbf{k}+\mathbf{q}}^{(l)}(\omega + i0^+, \omega + \nu + i0^+) \\ = 1 - r_{l+1} \Delta^2 G_{\mathbf{k}}^{(l+1)}(\omega) G_{\mathbf{k}+\mathbf{q}}^{(l+1)}(\omega + \nu) \\ \times \Gamma_{\mathbf{k}, \mathbf{k}+\mathbf{q}}^{(l+1)}(\omega + i0^+, \omega + \nu + i0^+), \end{aligned} \quad (6)$$

with  $r_l = l$  if  $l$  is even and  $r_l = (l+2)/9$  if  $l$  is odd, which is evaluated using Eq. (5) and  $\Gamma^{(L)} = 1$ . The lack of symmetry breaking is essential for a proper evaluation of the vertex [9,12] which, as long as the spin rotation invariance is intact, is reduced at most by  $\approx \frac{1}{3}$  for the high energy features. For lower excitation energies, this vertex is considerably enhanced for the hot quasiparticles; it is almost unaffected for the cold quasiparticles, reflecting again their qualitatively different behavior. We combine the results for  $G_{\mathbf{k}}(\omega)$  and the electron-spin fluctuation vertex function and so determine the irreducible spin susceptibility  $\tilde{\chi}_{\mathbf{q}}(\omega)$ . Assuming that  $\xi^{-1}(T) = \frac{1}{4} + \frac{1}{4} \frac{T-T_*}{T^{\text{cr}}-T_*}$  between  $T^{\text{cr}} = 470 \text{ K}$  and  $T_* = 220 \text{ K}$  and  $\xi^{-2}(T) = \frac{1}{4} + \frac{1}{7} \frac{T-T^{\text{cr}}}{700 \text{ K}-T^{\text{cr}}}$  above  $T^{\text{cr}}$  consistent with the NMR results of Curro *et al.* [2] for  $\text{YBa}_2\text{Cu}_4\text{O}_8$ , we find that both  $\tilde{\chi}_o(T)$  and  $\tilde{\chi}_Q(T)$  exhibit maxima at temperatures close to  $T^{\text{cr}}$  where  $\xi \approx 2$ . The falloff in  $\tilde{\chi}_o(T)$  and  $\tilde{\chi}_Q(T)$  below  $T^{\text{cr}}$  arises primarily from the transfer of quasiparticle spectral weight to higher energies. We find that both vertex corrections and the spectral weight transfer play a significant role in determining the low frequency spin dynamics. As may be seen in the inset of Fig. 2, when both effects are taken

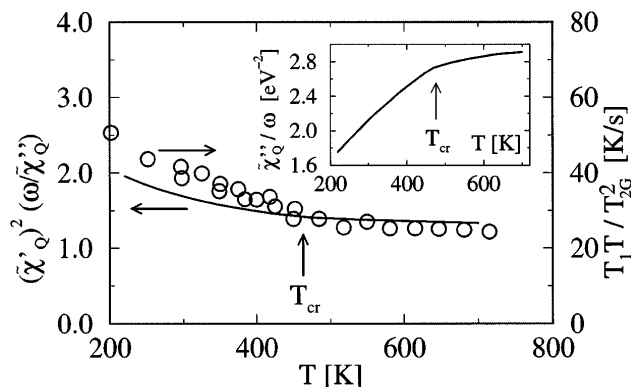


FIG. 2.  $\tilde{\chi}_Q''(\omega)/\tilde{\chi}_Q''(\omega)|_{\omega=0}$  as a function of temperature, compared with experimental results of Ref. [2] for  $T_1 T/T_{2G}^2$ . The inset shows the crossover in the calculated  $T$  dependence of  $\tilde{\chi}_Q''(\omega)/\omega|_{\omega=0}$ .

into account, our calculated values of the spin damping  $\gamma_Q = \tilde{\chi}_Q''(\omega, T)/\omega|_{\omega=0}$  display the crossover at  $T^{cr}$  anticipated by Monthoux and Pines [13]. Another calculable quantity which can be compared with experiment is  $\tilde{\chi}_Q(T)^2/\gamma_Q \equiv \omega_{sf}\chi_Q$ , being proportional to the product,  ${}^{63}T_1 T/({}^{63}T_{2G})^2$ . As may be seen in Fig. 2, qualitative agreement with the results of Curro *et al.* [2] for  $\text{YBa}_2\text{Cu}_4\text{O}_8$  is found. The determination of the full spin susceptibility  $\chi_q(\omega) = \tilde{\chi}_q(\omega)/[1 - J_q\tilde{\chi}_q(\omega)]$  is beyond the scope of the present work, since  $J_q$  is determined by the renormalization of the spin exchange fermion-fermion interaction through high energy excitations in all other channels. However, for  $\chi_o(T)$ , with  $J_{q=0}\tilde{\chi}_o(T_{cr}) = 0.5$ , a good quantitative fit to the experimental results of Curro *et al.* [2] between  $T^{cr}$  and  $T_*$  is found.

Physically, the most interesting aspect of our results is the appearance of SDW precursor phenomena, brought about by the strong interaction between the planar quasiparticles, for moderate AF correlation lengths,  $\xi > \xi_o \approx 2$ , in contrast to earlier calculations, in which SDW precursor behavior was found only in the limit of very large correlation length [14]. Our complete solution of the static problem enables us to access this region of strong coupling. For  $\xi > \xi_o$ , the hot electron mean free path,  $\sim \xi_o^2/\xi$ , begins to be small compared to  $\xi$ , so that the quasiparticle can no longer distinguish the actual situation from that of a SDW state; hence we find pseudo-SDW behavior, i.e., SDW behavior without symmetry breaking. The related shift of spectral weight for states close to  $(\pi, 0)$  affects mostly the low frequency part of the irreducible spin susceptibility and leads to the calculated crossover behavior.

The present theory cannot, of course, explain the leading edge pseudogap found below  $T_*$ , since one is then no longer in the quasistatic limit for which our calcula-

tions apply. Strong pseudogap behavior corresponds to a further redistribution of quasiparticle states lying within  $\approx 30$  meV of the Fermi energy. No appreciable change is seen in the high energy features found in the present calculations. It is likely that strong scattering in the particle-particle channel plays an increasingly important role below  $T_*$ , since we find above  $T_*$  important prerequisites for its appearance: an enhanced spin fluctuation vertex and a pronounced flattening of the dispersion of the hot quasiparticle states [15]. In addition, below  $T_*$  the quantum behavior of spin excitations becomes increasingly important, leading to the sizable suppression of the hot quasiparticle scattering rate found below  $T_*$  [7].

This work has been supported in part by the Science and Technology Center for Superconductivity through NSF Grant No. DMR91-20000, by the Center for Non-linear Studies at Los Alamos National Laboratory, and by the Deutsche Forschungsgemeinschaft (J.S.). We thank the Aspen Center for Physics for its hospitality during the period in which part of this paper was written, and Andrey V. Chubukov and Andrew J. Millis for helpful discussions.

- [1] V. Barzykin and D. Pines, Phys. Rev. B **52**, 13 585 (1995).
- [2] N.J. Curro, T. Imai, C.P. Slichter and B. Dabrowski, Phys. Rev. B **56**, 877 (1997).
- [3] A.G. Loeser *et al.*, Science **273**, 325 (1996); H. Ding *et al.*, Nature (London) **382**, 51 (1996).
- [4] P. Monthoux, A. Balatsky, and D. Pines, Phys. Rev. Lett. **67**, 3448 (1991); Phys. Rev. B **46**, 14 803 (1992).
- [5] P. Monthoux and D. Pines, Phys. Rev. B **47**, 6069 (1993); **48**, 4261 (1993).
- [6] A. Millis, H. Monien, and D. Pines, Phys. Rev. B **42**, 1671 (1990).
- [7] B.P. Stojković and D. Pines, Phys. Rev. Lett. **76**, 811 (1996); Phys. Rev. B **55**, 8576 (1997).
- [8] A.V. Chubukov, D. Pines, and B.P. Stojković, J. Phys. Condens. Matter **8**, 10 017 (1996).
- [9] A. Chubukov, D. Morr, and K.A. Shakhnovich, Philos. Mag. B **74**, 563 (1994); A. Chubukov and D. Morr, Phys. Rep. (to be published).
- [10] M.V. Sadovskii, Sov. Phys. JETP **50**, 989 (1979); J. Mosc. Phys. Soc. **1**, 391 (1991).
- [11] D.S. Marshall *et al.*, Phys. Rev. Lett. **76**, 4841 (1996).
- [12] For a discussion of the case of the symmetry broken state see J.R. Schrieffer, J. Low Temp. Phys. **99**, 397 (1995).
- [13] P. Monthoux and D. Pines, Phys. Rev. B **50**, 16 015 (1994).
- [14] A. Kampf and J.R. Schrieffer, Phys. Rev. B **42**, 7967 (1990).
- [15] A.V. Chubukov, e-print cond-mat/9709221; A.V. Chubukov and J. Schmalian, Phys. Rev. B (to be published).